COMPUTATIONAL METHODS FOR PREDICTING TAPERED HUB BEHAVIOR IN LARGE-DIAMETER, HIGH-PRESSURE VESSEL FLANGES

D.H. VAN CAMPEN,

Laboratory for Nuclear Engineering, Department of Mechanical Engineering, Delft University of Technology, Delft, The Netherlands

ABSTRACT

A comparison is offered between alternative computational methods for tapered hub behaviour in large-diameter, high-pressure vessel flanges occurring in literature, using a finite element analysis for reference. These existing methods consider the hub either as a thin cylindrical shell with linearly varying thickness or as a ring with undeformable radial cross section. An improved version of the thin shell approaches is presented for large values of the taper angle, while additionally the influence coefficients for the finite element approach are given in graphical form.

1. INTRODUCTION

Interest in the behaviour of high-pressure flanges has been stimulated by the advent of light-water-cooled and moderated nuclear reactors. The bolted flange joint between the pressure vessel head and body combines large size (typically, P.W.R. with inside vessel diameter $\approx$ 3.5 - 4.5 m for $\approx$ 155 bar internal pressure and B.W.R. with inside vessel diameter $\approx$ 5.5 - 6.5 m for $\approx$ 70 bar internal pressure) with unusually stringent leak-tightness requirement (typically, zero leakage past the outer O-ring during normal operation and transients). Fig. 1 shows the tapered hub design and metal-to-metal gasket aided by concentric metal O-rings typical for such flange joints.

The most significant difference between the type of flange joint shown and the more common low-pressure flanges concerns the flange ring thickness to width ratio, whose magnitude is of order unity for the high-pressure case while it is relatively small (say $\leq \sim 1/3$) for the low-pressure case. Therefore the (elastic) thin plate approach for the flange ring, underlying flange design according to the Divisions 1 and 2 of Section VIII of the ASME Boiler and Pressure Vessel Code [1], and developed in the classic paper by Waters, Wesstrom, Rossheim and Williams [2], cannot be utilized for the purpose of the present paper.

The (overall) behaviour of the flange connection is assumed to be elastic, thereby excluding methods of analysis which account for plastic hinges near the juncture between the flange and the vessel. These methods have been developed e.g. by Lake and Boyd [3] (thin plate approach for flange ring), underlying the British Code BS1500 [4], and by Siebel and Krägeloh [5] (rigid ring approach for flange ring), underlying the German Code [6]. They should be excluded for the large-diameter, high-pressure flanges of interest because of the

extremely stringent leak-tightness requirements mentioned before which enforce the deformation of the flange ring to be restricted within narrow limits.

Starting from a supposedly uniform distribution of bolt load, all methods commonly used in flange analysis assume both the loading and the geometry of the flange to be axisymmetric. The reliability of this approximation has been assessed by Menken [7] investigating an integral flange model without weakening through bolt holes and with concentrated bolt loads at the bolt pitch circle. From the numerical results given in [7] the important conclusion can be drawn that the influence of the local character of bolt loads on the average flange deformation pattern is negligibly small for the range of flange dimensions of interest for large-diameter, high-pressure vessels, i.e.

$$0.5 \leq \frac{t}{b_F} \leq 2.0; \quad \frac{b_F}{r_{cf}} \leq 0.3,$$

r_{cf} being the radius of the flange ring center of gravity circle, b_F the flange ring width and t the thickness of the flange ring (cf. Fig. 2).

On the basis of the axisymmetric character of loading and geometry, the general practice in deformation and stress analysis of pressure vessel flanges is to divide each member into its three constituent elements, i.e. ring, hub and shell (cf. Fig. 2). After determining the external loadings, the deformation of each of the three elements can be expressed in terms of the redundant shear forces and moments at their junctions. By applying the conditions of equilibrium and compatibility at the junctions, a set of simultaneous linear equations is obtained, which can be solved for the redundant forces and moments. Evaluation of the flange deformations is then a straightforward matter.

In determining the deformation of the separate elements the following schematizations are usual:

a. The flange ring is supposed to have an undeformable radial cross section . A rigorous numerical investigation carried out by Visser [8] on the basis of the finite element method for the representative case

$$\frac{t}{b_F} = 1.35 \; ; \quad \frac{b_F}{r_{cf}} = 0.19 \; ; \quad \frac{g_o}{r_o} = 0.06$$

showed, as one might expect, that this is a realistic assumption, except for a small region in the neighbourhood of the gasket face, where plastic deformation can be expected to occur. The implications of this local effect are discussed in [14]. Experimental results reported by Van Campen and Broekhoven [9] for the same case completely confirmed the numerical results.

b. The cylindrical or the spherical shell is treated by thin shell theory, using the Geckeler approximation [10] in the case of hemispherical head.

c. The tapered hub is considered either as a thin cylindrical shell with linearly varying thickness and a small taper [11, 12, 13] or as a ring with undeformable radial cross section [14]. Particularly for the tapered hub of the head flange shown in Fig. 1, the former approach may become doubtful because of the large taper and the short length of

the hub. At the same time this squat shape suggests the much simpler alternative of the latter approach. Section 2 therefore offers a comparison between these alternatives using a finite element analysis for reference.

2. TAPERED HUB BEHAVIOUR

In order to obtain a systematic approach and to restrict the number of geometric parameters during the basic phase of the flange analysis, the external flange loading has been replaced by two basic external loading components (Fig. 3), i.e. unit pressure loading p=1 and unit moment loading M=1. The unit pressure loading is in equilibrium with an equivalent external bolting force on the outside of the flange ring. This schematization is allowable because of the supposed rigid ring behaviour of the flange ring.
For the sake of brevity the present section restricts itself to the case that the taper hub flange is connected to a circular cylindrical shell.

The thin shell approach of the tapered hub used by Murray and Stuart [11] as well as in papers on tapered transition joints by Rodabaugh and Atterbury [12] and Hamada et al. [15] is based upon the solution given by Timoshenko [16, Chapter 15, Article 118] and Flügge [17, Chapter 5.5.3] for a thin shell with a circular cylindrical shape of the middle plane and a thickness varying linearly as a function of the axial hub co-ordinate. The same solution is used in the present paper, yielding the following expression for the radial displacement w (Fig. 2):

$$w = \frac{1}{\sqrt{\eta}} \left[C_1 \text{ ber}'(\xi) + C_2 \text{ bei}'(\xi) + C_3 \text{ ker}'(\xi) + C_4 \text{ kei}'(\xi)\right] + \frac{p r_o^2 (1-\nu/2)}{E\, \alpha\, \eta} \qquad (1)$$

where $\xi = 2\rho\sqrt{\eta}$, with $\rho = \sqrt[4]{\dfrac{12(1-\nu^2)}{\alpha^2 r_o^2}}$

while η is the axial hub co-ordinate defined in the figure.
In this solution ber' (ξ), bei' (ξ), ker' (ξ) and kei' (ξ) represent the derivatives of the so-called Thomson functions with respect to η. The end rotations ϕ_o and ϕ_1, the end moments M_o and M_1 and the end shear forces Q_o and Q_1 can be expressed in the integration constants C_1 through C_4, considering that:

$$\phi = \frac{dw}{d\eta}\ ;\quad M = \frac{Eg^3}{12(1-\nu^2)} \frac{d^2w}{d\eta^2}\ ;\quad Q = \frac{d}{d\eta}\left[\frac{Eg^3}{12(1-\nu^2)} \frac{d^2w}{d\eta^2}\right] \qquad (2)$$

At this point the critical stage in the thin shell approach is reached, where the continuity conditions at the hub boundaries have to be satisfied. In satisfying these conditions Murray and Stuart in their classic paper on the behaviour of large taper hub flanges [11] assume the pressure forces (stress resultants) at the cylindrical shell and the flange ring junctures to act parallel with the vessel axis and to have their points of application in the hub middle surface. However, this is not consistent with the basic thin shell solution mentioned above, as the conical shape of the middle plane, i.e. the difference between the radii $r_i + g_o/2$ and $r_i + g_1/2$, produces an additional moment increasing with η (cf. Fig. 2)

along the axial length of the hub. As indicated by the experimental evidence presented in [12], this effect becomes quite significant for g_1/g_o ratios exceeding about 1.5 and $h/\sqrt{r_o g_o}$ values not exceeding about 2 $\sqrt{2}$, i.e. for hub dimensions relevant in the context of the present paper. To take this effect into account both the analyses given in [12] and [15] assume the pressure forces at the cylindrical shell and the flange ring junctures to be located in the conical hub middle surface, thereby introducing a radial shear force at each of these junctures. In order to assess the reliability of this correction the present section offers a comparison between the two approaches mentioned above and simultaneously offers a third approach where the shape of the hub middle surface is assumed to be cylindrical in satisfying the continuity conditions. The system of 8equations resulting from the continuity conditions at the hub boundaries for the latter case has been presented in tabulated form in Table 1 of [14].

The alternative approach mentioned before is to treat the hub as a ring with undeformable cross section, i.e., in the same way as the flange ring. This results in two separate modes of deformation undergone by the hub: (1) rotation of the cross section around the centroid due to the resultant twisting moment M_{wh} and (2) radial displacement of the cross section due to the resultant radial force through the centroid (both M_{wh} and Q_h are measured per unit arc length in circumferential direction of the cylindrical shell midsurface). The system of four equations for the redundant shear forces and moments Q_o, Q_1, M_o and M_1, resulting from the continuity conditions at the hub boundaries for this case has been tabulated in Table 2 of [14].

The final part of this section offers a comparison between the three thin shell approaches and the rigid ring approach for the tapered hub discussed before, using a finite element analysis as the yardstick for their validity. The finite element approach utilizes the so-called ana-element concept for the flange ring and the cylindrical vessel. This concept, which has been introduced systematically by the author [18], enables to evaluate element stiffness matrices on the basis of known analytical solutions of the elasticity equations. The elements used in the finite element approach for the description of the tapered hub behaviour are the TRIAX 6 elements developed by Argyris [19]. The displacement continuity conditions at the flange ring and vessel boundaries in this approach are satisfied by prescribing the hub edge displacements to be distributed linearly across the wall thickness. A flowchart of the general computer program underlying the numerical investigations is shown in Fig. 4.

The calculations have been carried out for the representative case

$$\frac{t}{b_F} = 1.25 \; ; \quad \frac{b_F}{r_{cf}} = 0.2 \; ; \quad \frac{g_o}{r_o} = 0.05$$

The results of the comparison are given in Fig. 6 for unit moment loading (representative for tightening conditions) and in Fig. 7 for representative operating conditions. The additional assumptions for some geometrical and loading parameters for the latter loading case are indicated in the figure. The results are presented in terms of the flange ring rotation as a function of g_1/g_o for several values of the dimensionless parameter $\sqrt{r_o g_o}/h$, covering the range of practical interest (i.e. $\sqrt{r_o g_o}/h = 1, 2, 4, 8$).

It may be concluded from these figures that the thin shell approach developed by Rodabaugh and Atterbury [12] and utilized by Hamada et al. [13, 15] gives the best results over nearly the whole range of these two dimensionless parameters. However, for relatively large values of $\sqrt{r_o g_o}/h$ and correspondingly large values of g_1/g_o, i.e. for large values of the taper angle α (i.e. $\alpha \geq \sim 55^o$), the approach considering the hub middle surface to be cylindrical in satisfying the continuity conditions gives the most accurate values for the flange ring rotation.

As regards the validity of the rigid ring approach for the hub, Fig. 8 shows the boundaries in the g_1/g_o - $\sqrt{r_o g_o}/h$ - plane where the relative deviation of the rigid ring approach from the finite element approach under tightening conditions and operating conditions equals 5% and 10% respectively.

As can be seen from Fig. 4 an additional output obtainable from the finite element computations is formed by the influence coefficients for the tapered hub. These influence coefficients can be used by design engineers who do not have, in general, finite element programs at their disposal in a very easy way for including tapered hub behaviour in deformation analysis of flanges. Therefore they are presented in graphical form in the next section.

3. INFLUENCE COEFFICIENTS FOR THE TAPERED HUB CONSIDERED AS AN ASSEMBLAGE OF TRIAX 6 ELEMENTS

In this section the influence coefficients will be presented for the tapered hub considered as an assemblage of TRIAX 6 elements. At first glance, one would think that these influence coefficients should refer to the hub boundary loadings Q_o, M_o, Q_1 and M_1 shown in Fig. 2 and the edge deformations w_o, ϕ_o, w_1 and ϕ_1 resulting therefrom. However, in that case these influence coefficients can be shown to depend on the three dimensionless parameters

$$\frac{g_o}{r_o}, \quad \frac{g_1}{g_o} \quad \text{and} \quad \sqrt{r_o g_o}/h$$

A closer inspection of the equations underlying the thin shell analysis discussed in section 2 reveals that appropriately defined influence coefficients only depend on the two dimensionless parameters g_1/g_o and $\sqrt{r_o g_o}/h$. As the thin shell behaviour of the tapered hub has been shown to be dominant in the preceding section it can be stated with sufficient accuracy from a practical point of view that these influence coefficients will also only depend on the above two parameters for the case that the hub is considered as an assemblage of TRIAX 6 elements. The modified influence coefficients $\overline{\alpha_{ij}} = \alpha_{ji}$ (i=1,.., 4, j=1,.., 4) are defined as follows

$$w_o = \frac{1}{E}\left[\frac{r_o}{g_o}\right]^2 \left[-\alpha_{11}\, Q_o \sqrt{\frac{g_o}{r_o}} + \alpha_{12}\frac{M_o}{r_o} - \alpha_{13}\, Q_1 \sqrt{\frac{g_o}{r_o}} - \alpha_{14}\frac{M_1}{r_o}\right] + \alpha_{1p}\frac{p\, r_o^2}{E\, g_o}, \tag{3}$$

$$\sqrt{r_o g_o}\,\phi_o = \frac{1}{E}\left[\frac{r_o}{g_o}\right]^2 \left[-\alpha_{21}\, Q_o \sqrt{\frac{g_o}{r_o}} + \alpha_{22}\frac{M_o}{r_o} - \alpha_{23}\, Q_1 \sqrt{\frac{g_o}{r_o}} - \alpha_{24}\frac{M_1}{r_o}\right] + \alpha_{2p}\frac{p\, r_o^2}{E\, g_o}, \tag{4}$$

$$w_1 = \frac{1}{E}\left[\frac{r_o}{g_o}\right]^2 \left[\alpha_{31}\, Q_o \sqrt{\frac{g_o}{r_o}} - \alpha_{32}\frac{M_o}{r_o} + \alpha_{33}\, Q_1 \sqrt{\frac{g_o}{r_o}} + \alpha_{34}\frac{M_1}{r_o}\right] + \alpha_{3p}\frac{p\, r_o^2}{E\, g_o}, \tag{5}$$

$$\sqrt{r_o g_o}\,\phi_1 = \frac{1}{E}\left[\frac{r_o}{g_o}\right]^2 \left[-\alpha_{41}\, Q_o \sqrt{\frac{g_o}{r_o}} + \alpha_{42}\frac{M_o}{r_o} - \alpha_{43}\, Q_1 \sqrt{\frac{g_o}{r_o}} - \alpha_{44}\frac{M_1}{r_o}\right] + \alpha_{4p}\frac{p\, r_o^2}{E\, g_o}, \tag{6}$$

where α_{1p}, α_{2p}, α_{3p} and α_{4p} are proportional to the free edge deformations due to the internal loading (including the axial pressure force) acting on the tapered hub. The modified influence coefficients are given in graphical form in Fig.s 9 through 13 as a function of g_1/g_o for several values of $\sqrt{r_o g_o}/h$ (i.e. $\frac{\sqrt{r_o g_o}}{h} = \frac{1}{2}, 1, 2, 4, 8$) and intend to cover the range of practical interest. In order to obtain a systematic presentation the coefficients α_{1p} and α_{3p} have been replaced by $\frac{1}{2}[\alpha_{1p} + \alpha_{3p}]$ and $[\alpha_{1p} - \alpha_{3p}]\frac{\sqrt{r_o g_o}}{h}$. For values of $\sqrt{r_o g_o}/h$ between the values mentioned above the influence coefficients can be obtained via interpolation.

4. CONCLUSIONS

The thin shell approach for the tapered hub developed by Rodabaugh and Atterbury [12] and utilized by Hamada et al. [13, 15] gives the most accurate values for the flange ring rotation, except for large values of the taper angle α (i.e. $\alpha \geq \sim 55^{\circ}C$), where the approach proposed by the author [14] gives the best results. However, this latter approach also gives results within sufficiently accuracy from a practical point of view for other values of α.
The thin shell approach used by Murray and Stuart [11] underestimates the flange ring rotation considerably, particularly for relatively large values of the taper angle.
The rigid ring approach for the tapered hub only gives accurate results for the flange ring rotation within a very restricted range of the dimensionless hub geometry parameters (cf. Fig. 8).

ACKNOWLEDGEMENT

The author wishes to thank Professor D.G.H. Latzko for useful suggestions during the investigations that are part of his doctor's thesis at the Laboratory for Nuclear Engineering of the Delft University of Technology.

REFERENCES

[1] American Society of Mechanical Engineers; Division 1 (Pressure Vessels) and Division II (Alternative Rules for Pressure Vessels) of Section VIII of the ASME Boiler and Pressure Vessel Code; ASME United Engineering Center, New York, 1968.

[2] Waters, E.O., Wesstrom, D.B., Rossheim, D.B. and Williams, F.S.G.; Formulas for stresses in bolted flanged connections; Trans. ASME, Fuel and Steam Power, Vol.59, no.4, 1937, pp. 161-169.

[3] Lake, G.F. and Boyd, G.; Design of bolted, flanged joints of pressure vessels; Proc. Inst. Mech. Engrs., Vol.171, 1957, pp. 843-858.

[4] British Standards Institution; B.S. 1500, Part I; 1958.

[5] Siebel, E. and Krägeloh, E.; Untersuchungen an Dichtungen für Rohrleitungen; Konstruktion, no.7, 1955, pp. 123-137 and pp. 187-196.

[6] Arbeitsgemeinschaft Druckbehälter; AD-Merkblätter.

[7] Menken, C.M.; Influence of bolt loading on deformation of pressure vessel flanges; Proc. First Int. Conf. on Pressure Vessel Technology, Delft, Sept.29-Oct.2, 1969, Part I Design and Analysis, paper I-11, pp. 143-153.

[8] Visser, W.; Calculation of flange deformation of Dodewaard reactor vessel by means of finite elements (in Dutch); Report MORS-Ad-1, Lab. for Nuclear Engineering, Delft Un. of Technology, 1968.

[9] Campen, D.H. van and Broekhoven, M.J.G.; Final report concerning stress and strain analysis on models of the Dodewaard reactor pressure vessel (in Dutch), Parts I, II and III; reports Lab. for Nuclear Engineering, Delft Un. of Technology, 1968.

[10] Geckeler, J.W.; Über die Festigkeit achsensymmetrischer Schalen; Forschungsarbeiten auf den Gebiete des Ingenieurwesen; Vol.276, Berlin 1926.

[11] Murray, N.W. and Stuart, D.G.; Behaviour of large taper hub flanges; Proc. Symposium on Pressure Vessel Research towards Better Design, Inst. Mech. Eng., London, 1962, pp. 133-147.

[12] Rodabaugh, E.C. and Atterbury, T.J.; Stresses in tapered transition joints in pipelines and pressure vessels; J. Eng. Indus., Trans. ASME, series B, vol.84, 1962, pp. 321-328.

[13] Hamada, K, Ukaji, H. and Hayaski, T.; Stress analysis of bolted flanges for pressure vessels; Proc. First Int. Conf. on Pressure Vessel Technology, Delft, Sept.29-Oct.2, 1969, Part I Design and Analysis, paper I-42, pp. 513-525.

[14] Campen, D.H. van, Deen, P.J. and Latzko, D.G.H.; Deformation of large-diameter, high-pressure vessel flanges; Proc. First Int. Conf. on Pressure Vessel Technology, Delft, Sept.29-Oct.2, 1969, Part I Design and Analysis, paper I-43, pp. 529-549.

[15] Hamada, K., Hayaski, T. and Oguchi, I.; Stress analysis of tapered transition joints in reactor pressure vessel; report ORNL-tr-1769, 1966, distributed by Clearinghouse, U.S. Department of Commerce.

[16] Timoshenko, S.P., Woinowsky-Krieger, S.; Theory of plates and shells; Second edition, Mc.Graw-Hill, New York, Toronto, London, 1959.

[17] Flügge, W.; Stresses in shells; Springer-Verlag, Berlin/Göttingen/Heidelberg, second edition, 1962.

[18] Campen, D.H. van; Some applications of engineering mechanics in pressure vessel analysis; Thesis Delft Un. of Technology (to be published).

[19] Argyris, J.H.; The TRIAX 6 element for axisymmetric analysis by the matrix displacement method, Part I Foundations; The Aeronautical Journal of the Royal Aeronautical Society, Vol.70, Dec. 1966, pp. 1102-1105.
Argyris, J.H.; The TRIAX 6 element for axisymmetric analysis by the matrix displacement method, Part II Elastic stiffness and influence of initial strains; The Aeronautical Journal of the Royal Aeronautical Society, Vol.70, Dec. 1966, pp. 1105-1106.

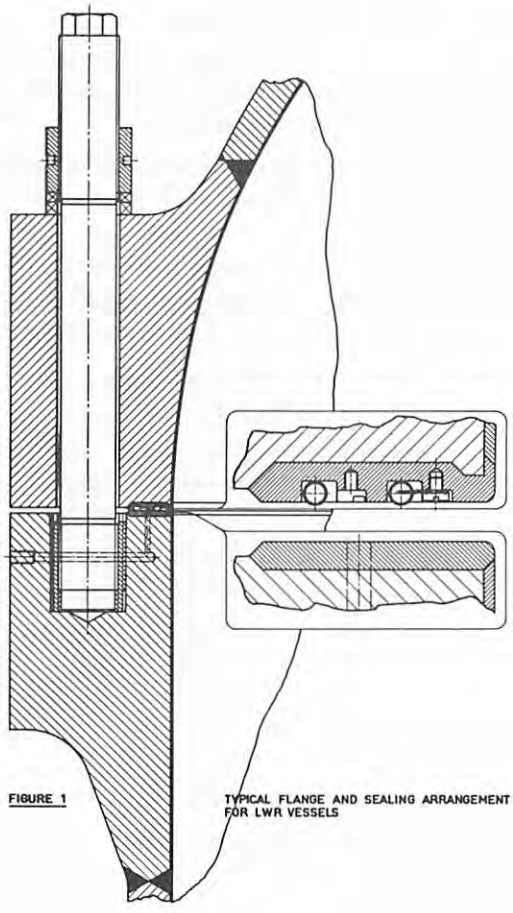

FIGURE 1 TYPICAL FLANGE AND SEALING ARRANGEMENT FOR LWR VESSELS

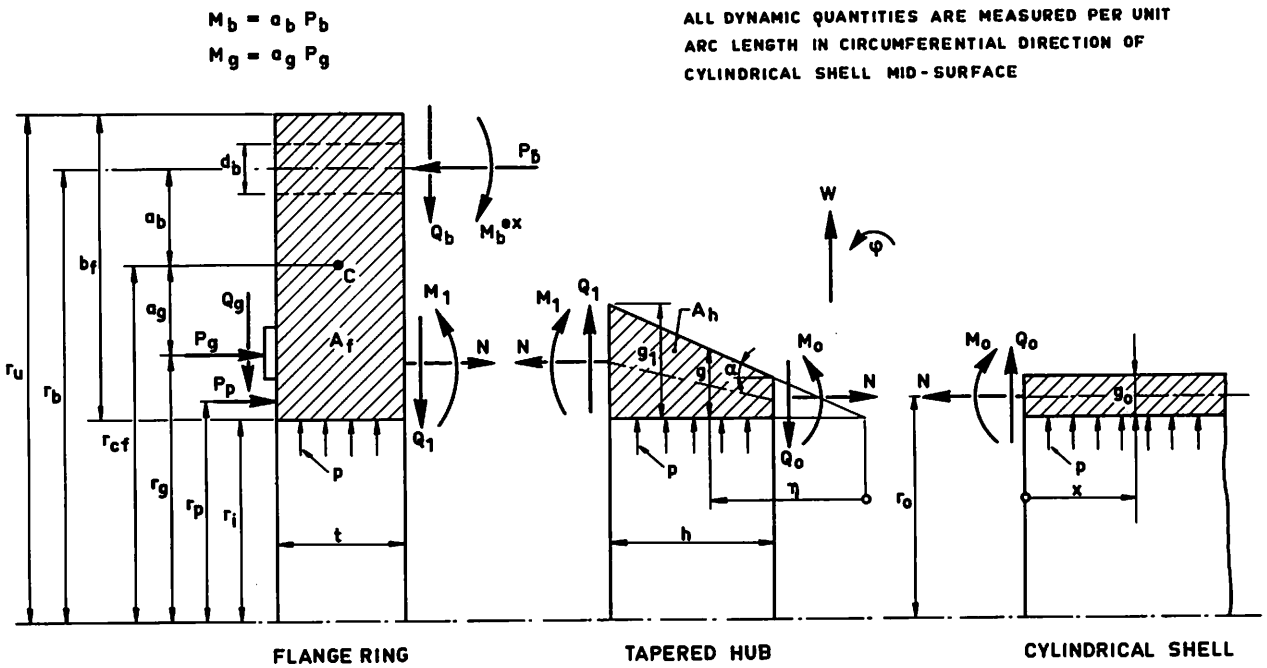

FIG.2. CONSTITUENT ELEMENTS WITH IN-AND EXTERNAL LOADING

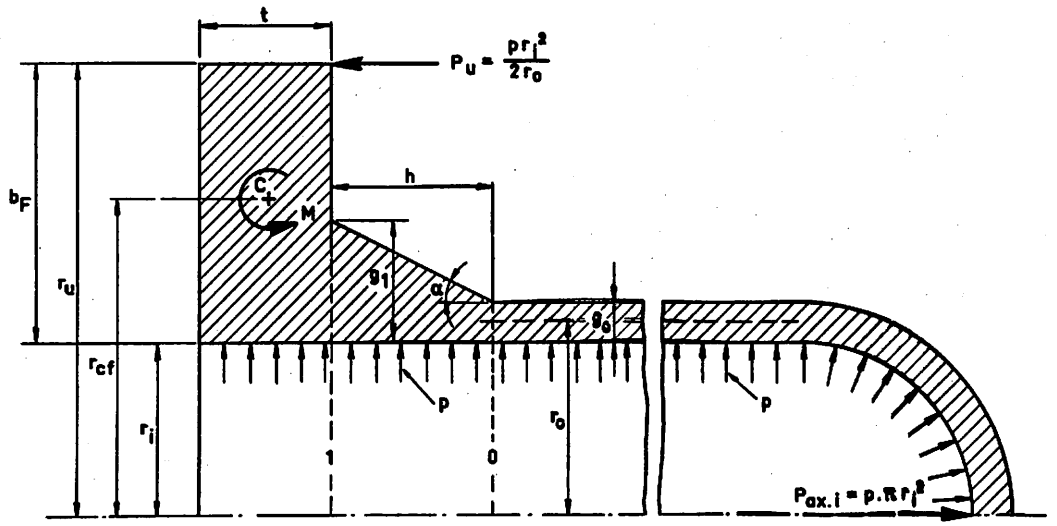

FIG. 3. EQUIVALENT EXTERNAL LOADING

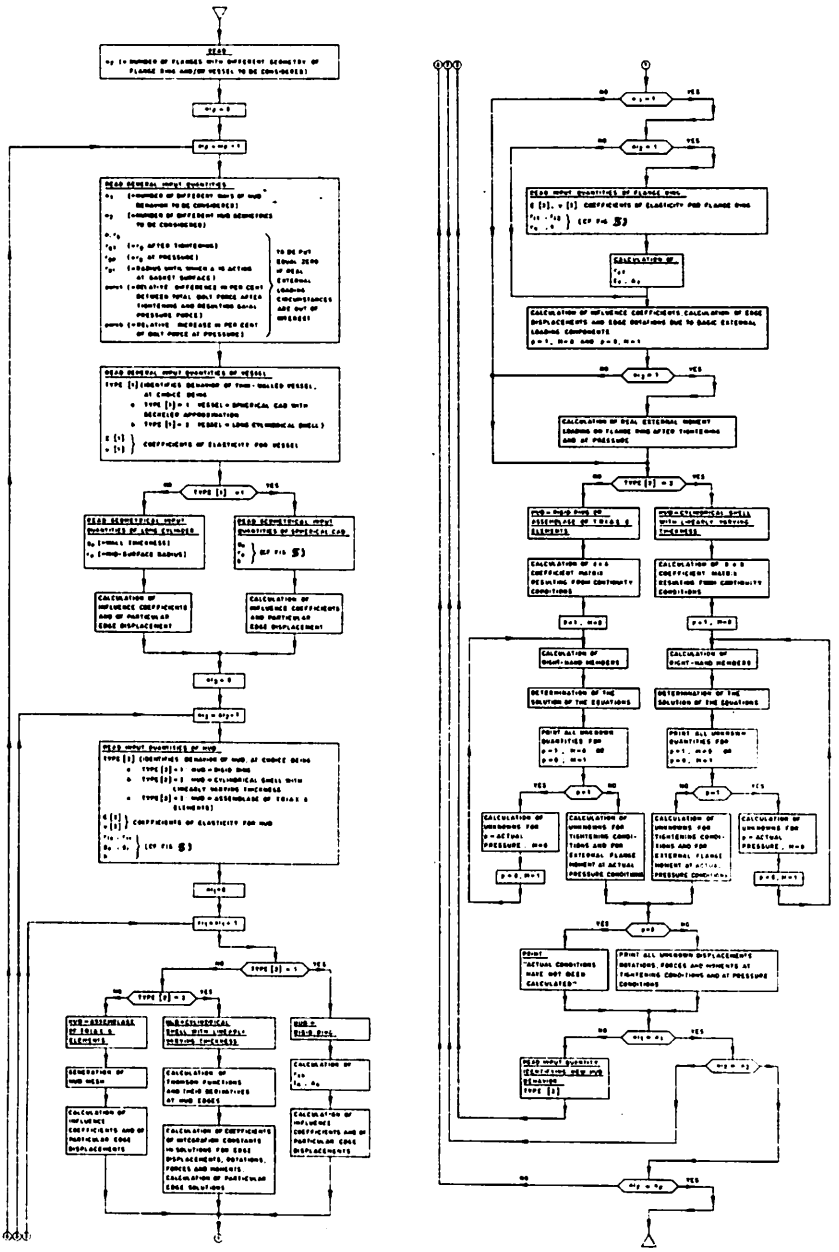

FIG. 4. FLOWCHART OF GENERAL COMPUTER PROGRAM FOR FLANGE ANALYSIS UNDER MECHANICAL LOADING.

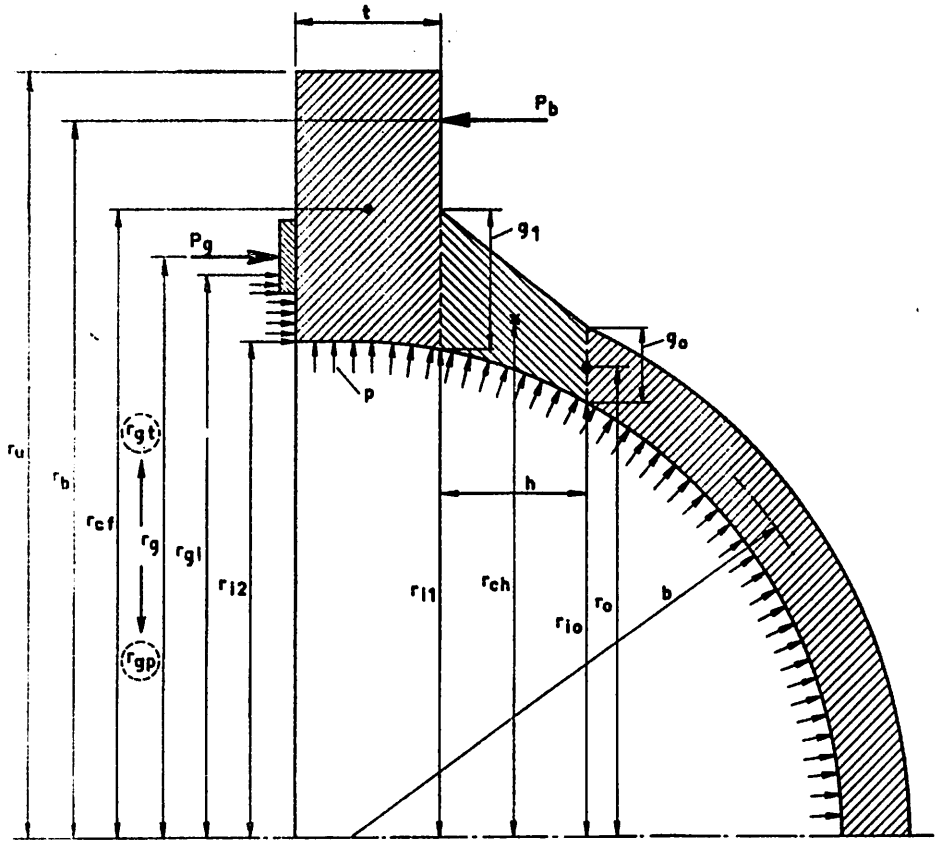

FIG. 5. FLANGE GEOMETRY SYMBOLS

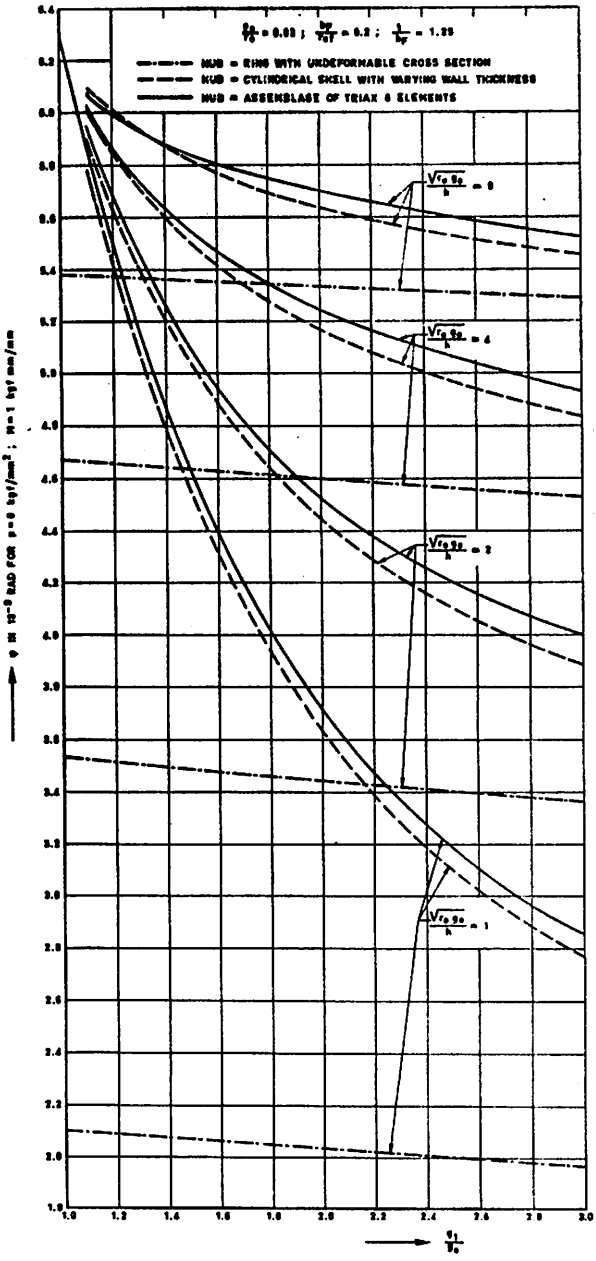

FIG. 6. FLANGE ROTATION FOR UNIT MOMENT LOADING

($\frac{\sqrt{r_0 g_0}}{h} = 1, 2, 4$ AND 8)

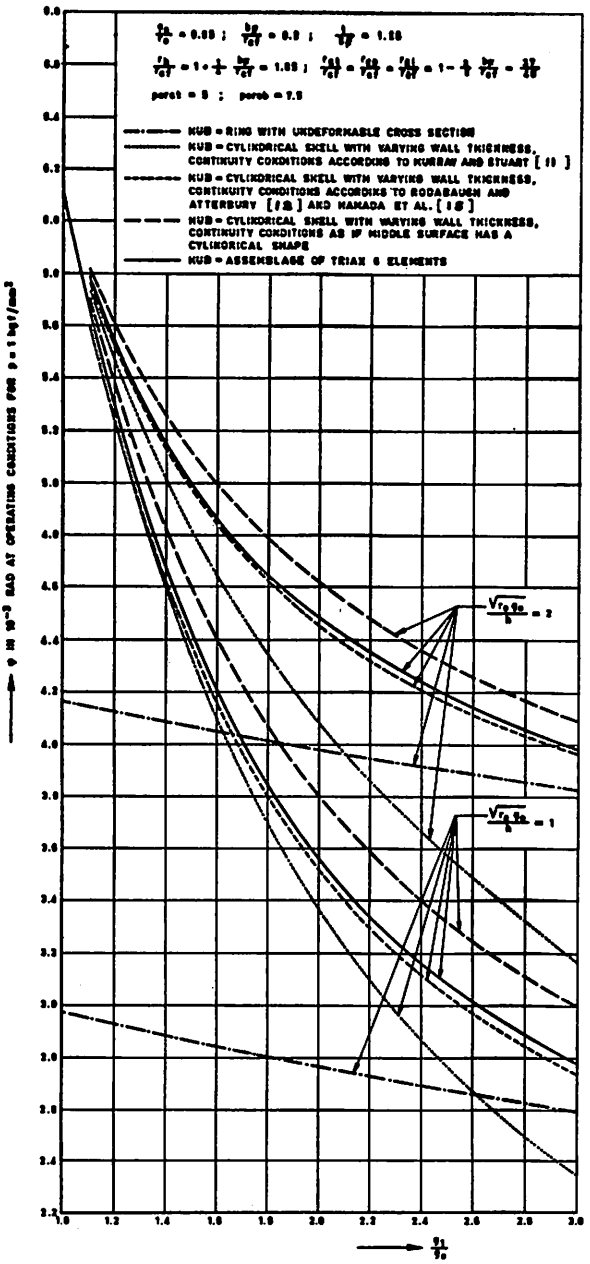

FIG. 7A. FLANGE ROTATION FOR OPERATING CONDITIONS ($\frac{\sqrt{r_o g_o}}{h}$ = 1 AND 2)

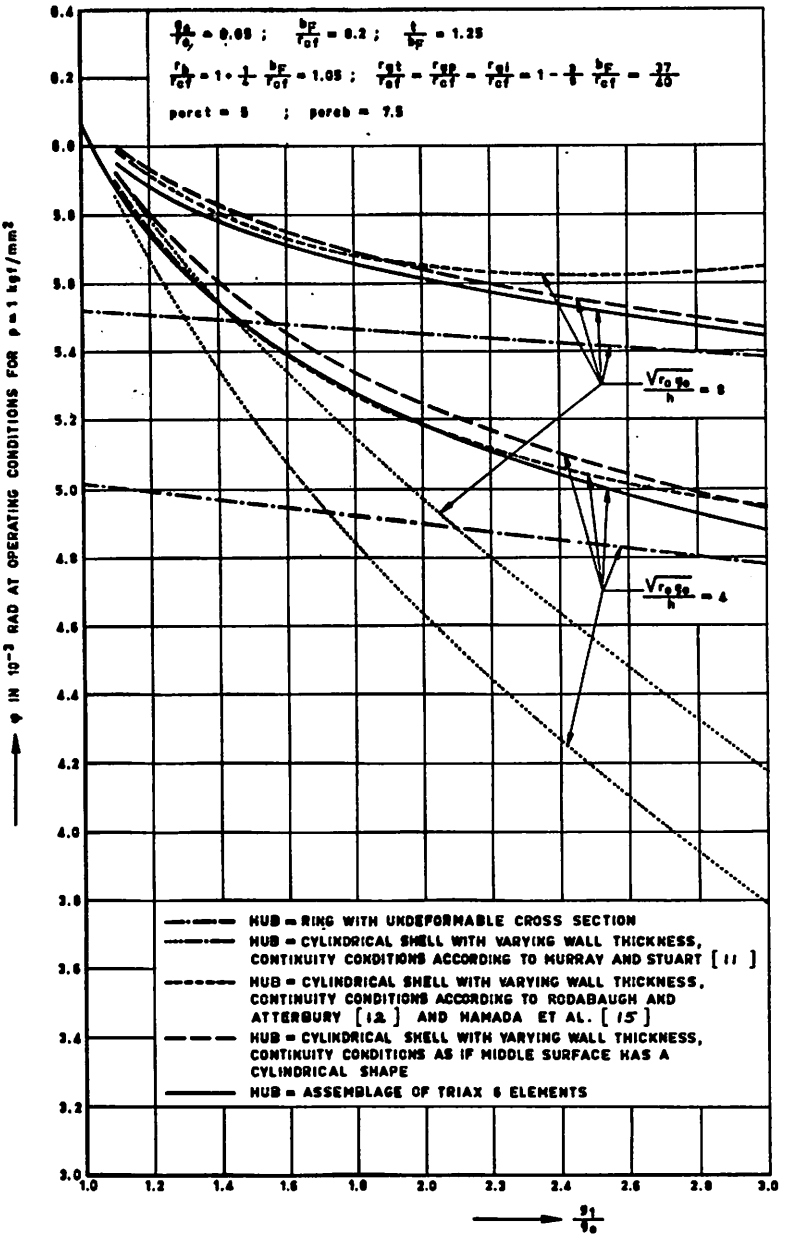

FIG. 7.8. FLANGE ROTATION FOR OPERATING CONDITIONS ($\frac{\sqrt{r_0 g_0}}{h}$ = 4 AND 8)

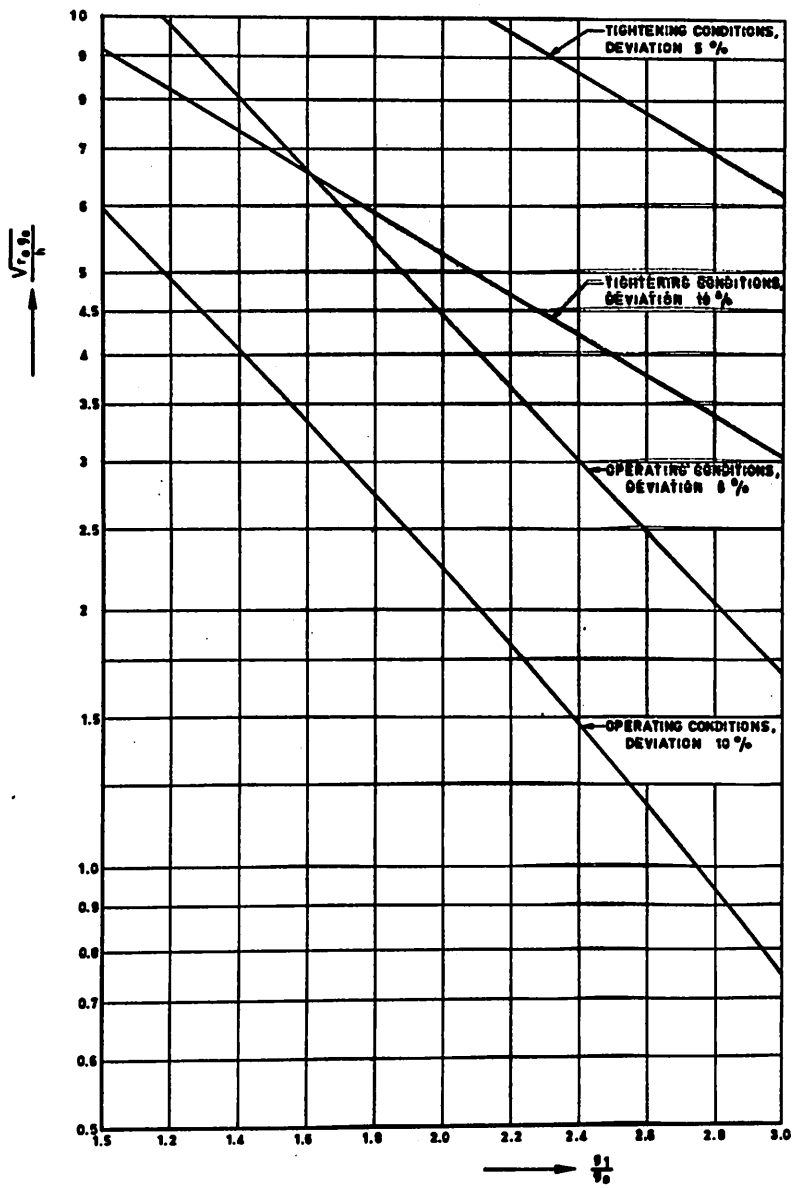

FIG. 6. VALIDITY RANGE FOR RIGID RING APPROACH OF TAPERED HUB.

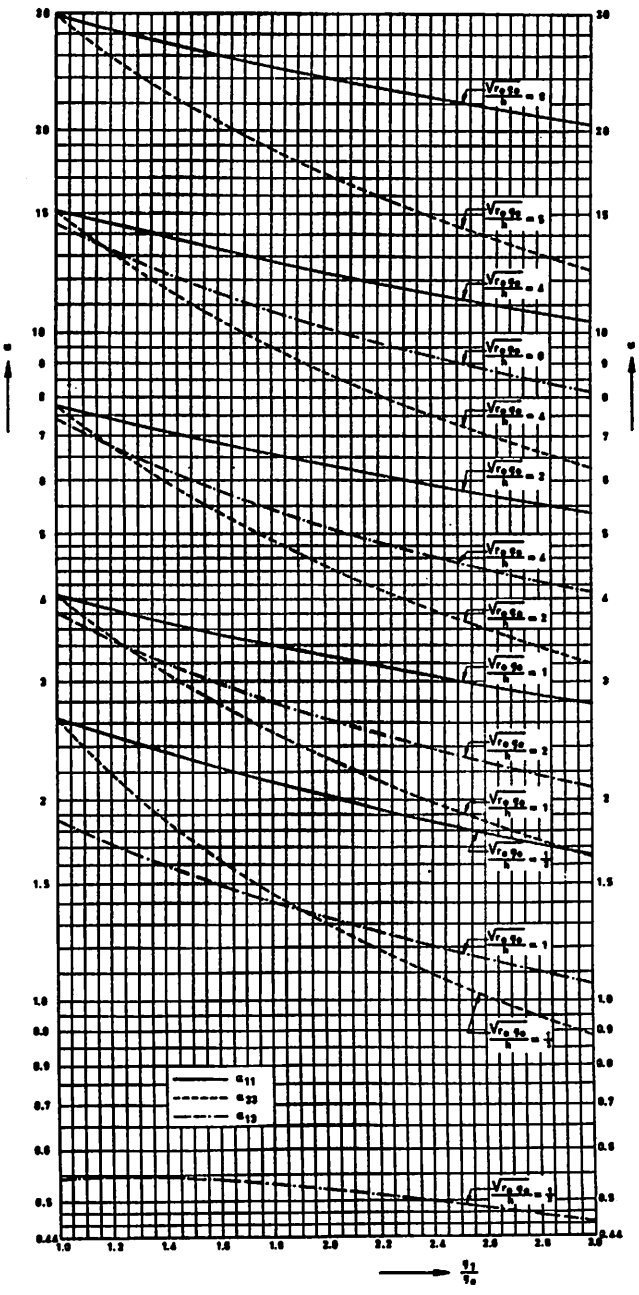

FIG. 8. THE INFLUENCE COEFFICIENTS a_{11}, a_{33} AND a_{13}

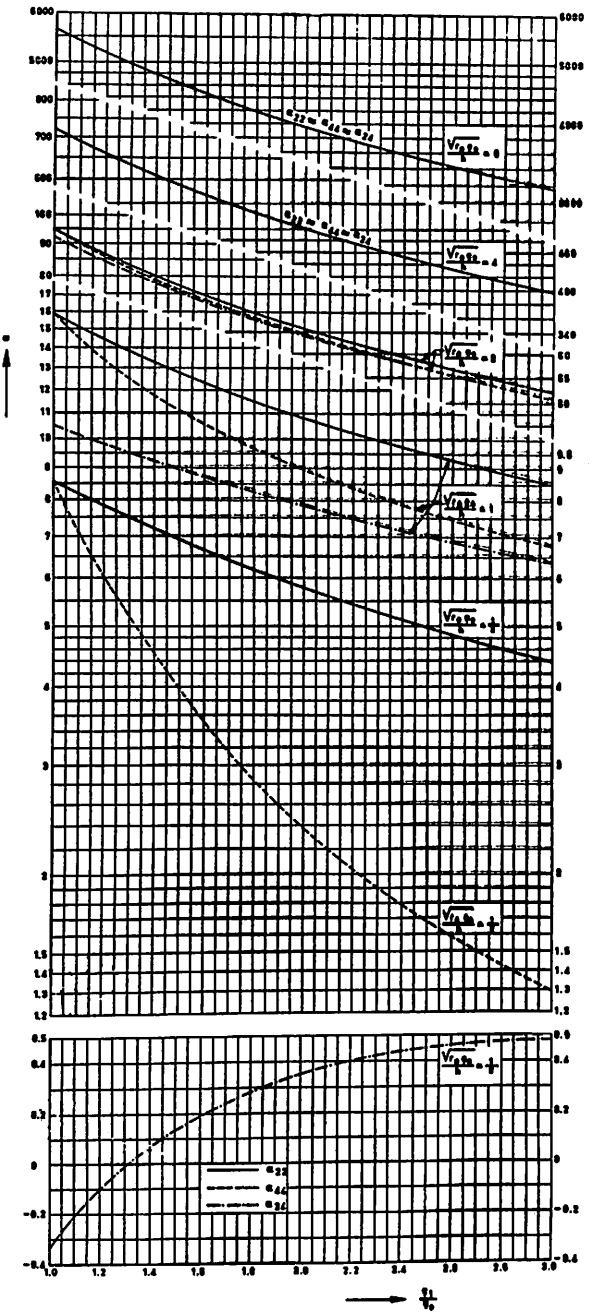

FIG. 10. THE INFLUENCE COEFFICIENTS a_{22}, a_{44} AND a_{24}

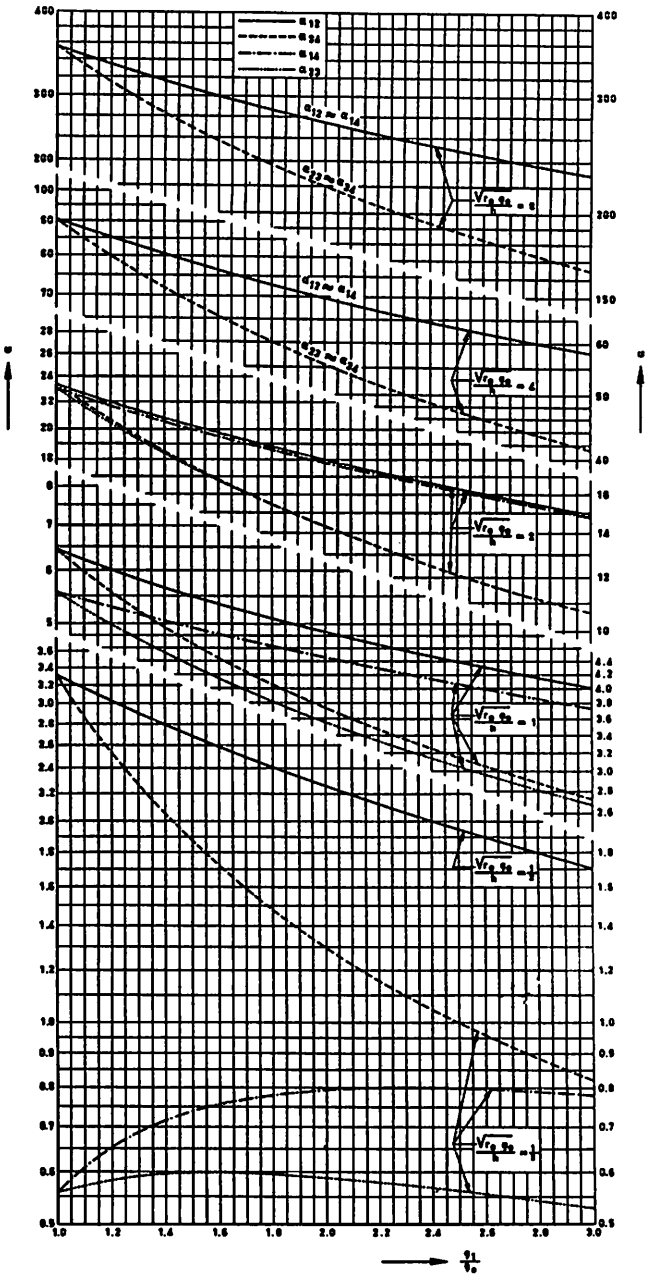

FIG. 11. THE INFLUENCE COEFFICIENTS a_{12} , a_{34} , a_{14} AND a_{33}

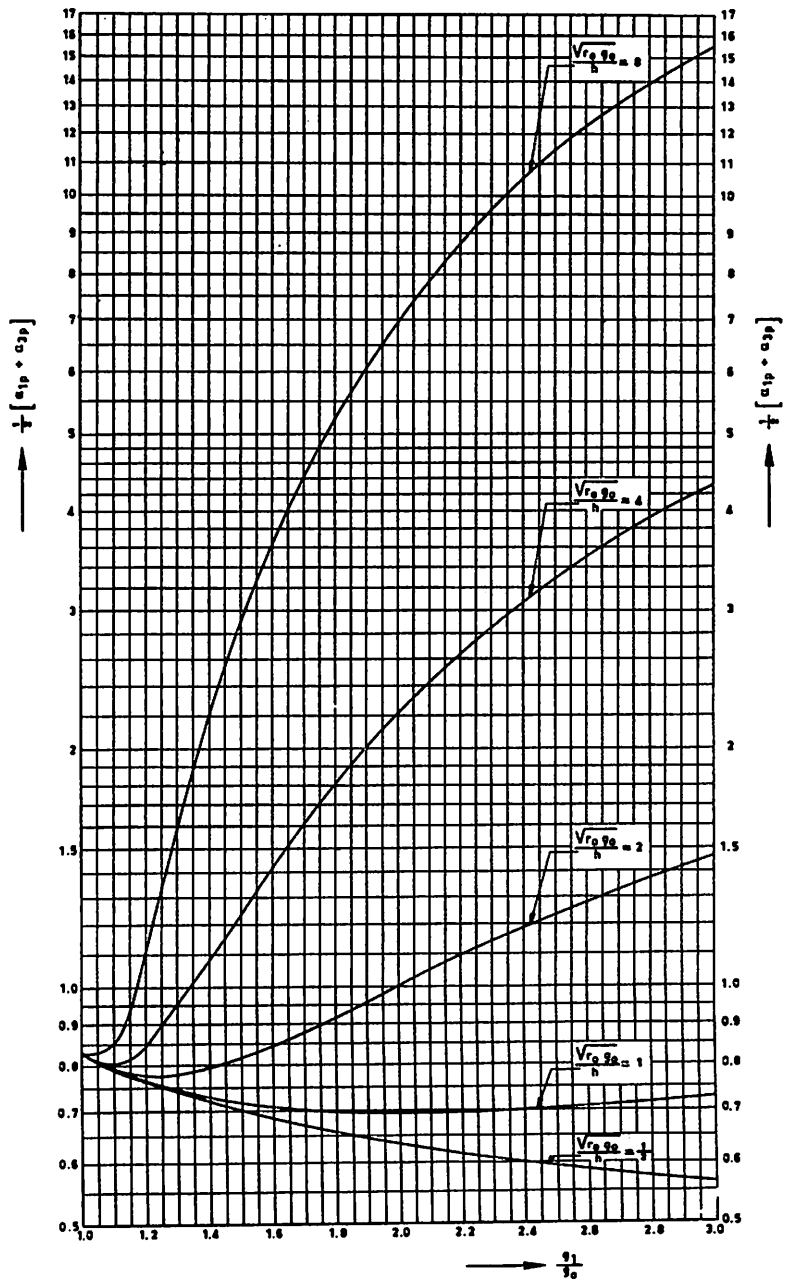

FIG. 12. THE COEFFICIENT $\frac{1}{7}[a_{1p} + a_{3p}]$

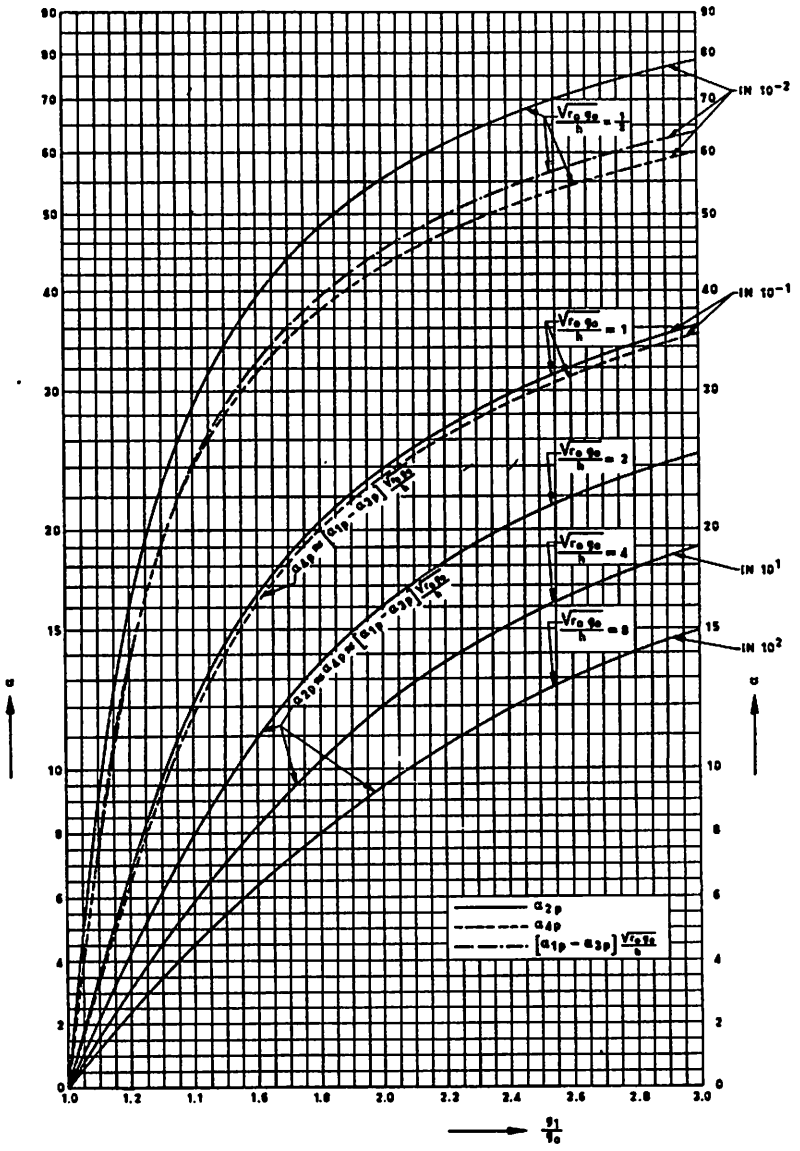

FIG. 13. THE INFLUENCE COEFFICIENTS α_{2p}, α_{4p} AND $[\alpha_{1p} - \alpha_{3p}] \frac{\sqrt{r_o q_o}}{h}$

DISCUSSION

Q J. G. LEKKERKERKER, The Netherlands

1. Your problem concerns the determination of the rotation of the flange ring which is important in view of the tightness of the flange connection. It seems to me that the local stress problem near the gasket is of at least equal importance. As far as I know no work about that has been reported at this conference.
2. Don't you think that the cost of a computer program in order to treat the hub using finite element methods is negligibly small as compared with the total cost of a nuclear power plant, which makes it highly improbable that a designer would not have this facility at his disposal ?

A D. H. VAN CAMPEN, The Netherlands

1. This is indeed true. Due to the combination of geometrical and physical non-linearities it is hardly possible to get theoretical information on this problem. Some first experimental evidence was presented at the 1969 Delft conference by our laboratory. We are now comparing this evidence with the theoretical results obtained from the program discussed in the paper.
2. Of course this is true for nuclear power plants, but the method presented also holds for non-nuclear flanges where it generally is not. On the other hand still quite a lot of design engineers in the nuclear field do not have finite element programs at their disposal.